minerals

MDPI

Article

Mineralogical Characteristics of Early Permian Paragonite-Bearing Coal (No. 3) in the Jinyuan Mine, Tengxian Coalfield, Shandong Province, Eastern China

Wenmu Guo [1], Jinxiao Li [1], Zhenzhen Wang [1], Ke Zhang [1], Zheng Gao [1], Jialiang Ma [2] and Cunliang Zhao [1,*]

1 Key Laboratory of Resource Exploration Research of Hebei Province, Hebei University of Engineering, Handan 056038, China; gwm1992313@126.com (W.G.); lijinxiao1010@163.com (J.L.); wzz90620512@163.com (Z.W.); Zhangke9801@163.com (K.Z.); gz326650578@163.com (Z.G.)

2 Institute for Atmospheric and Environmental Sciences Faculty of Geoscience and Geography, Goethe-University Frankfurt, 60438 Frankfurt, Germany; ma@iau.uni-frankfurt.de

* Correspondence: zhaocunliang@hebeu.edu.cn

Received: 24 July 2020; Accepted: 10 August 2020; Published: 12 August 2020

check for updates

Abstract: The Early Permian coal is of great value in the Tengxian Coalfield, Shandon Province, Eastern China. This work deals with the new data focusing on mineralogical characteristics in the Early Permian Shanxi Formation No. 3 coal from the Jinyuan Mine. The Jinyuan coal is a low ash and highly volatile A bituminous coal. Minerals in the No. 3 coal mainly comprise of kaolinite, ankerite, illite, calcite, siderite, and quartz, with varying compositions of trace amounts of pyrite, jarosite, bassanite, anatase, and rutile. According to mineral assemblage in the coal plies, three Types (A to C) can be identified in the No. 3 coal. The dominant minerals in Type A are poorly-ordered kaolinite, illite, quartz, pyrite, and jarosite. Type B is mainly composed of well-ordered kaolinite, illite, siderite, ankerite, and calcite. Type C, with just one sample (JY-3-7c), which contains high proportions of calcite (54%) and ankerite (34%). Terrigenous minerals are elevated in coal plies that typically have relatively high contents of ash yield. The formation of syngenetic pyrite was generally due to seawater, while the sulphate minerals (jarosite and coquimbite) were derived from the oxidation of pyrite. Epigenetic vein-like or fracture-fillings carbonate minerals (ankerite, calcite, and siderite), kaolinite, and pyrite, as well as authigenic quartz were derived from the influx of hydrothermal fluids during different periods, from the authigenic to epigenetic. The paragonite in the coal may have been formed by the precipitated from Na-rich hydrothermal fluids. No effects of magmatic intrusion on mineralogy were investigated in this research.

Keywords: Early Permian; coal; minerals; terrigenous; hydrothermal fluids; seawater influence

1. Introduction

Coal is an irreplaceable economic resource and still used as an electrical energy source, supplying the major global electricity needs around the world [1,2], especially in China, which has consumed large amounts of coal in recent years (for instance, amounting to 4.73 Gt in 2018) [3,4].

Coal is a kind of sedimentary rock and is mainly composed of organic ingredients (or macerals) and inorganic compositions [5–8], the latter of which consists of discrete crystalline particles, amorphous mineral phases, and non-mineral inorganic elements [7,8]. The study of the minerals in coal is of great significance, not only because it can be used as a critical indicator to understand the peat depositional conditions and various geologic processes during the whole period of coal formation [7,9–11], but also because it can solve practical problems (e.g., abrasion, stickiness, and corrosion) that are caused by minerals during coal utilization [7,8,12–14]. Furthermore, numerous researchers have also paid great attention to the adverse pollution and health-related effects produced as a result of minerals during coal combustion and utilization [15–23], such as acid rain and endemic diseases caused by coal combustion [15,19–21]. Therefore, it is necessary to investigate the mineralogical anomalies of minerals in coals.

The Early Permian coal is of great significance as a resource in North China, especially in Southwestern Shandong Province. It contains many large coalfields, such as Juye, Yanzhou, Tengxian, and others, making it an indispensable energy resource base for Shandong Province. However, after the Carboniferous–Permian periods, frequent and intensive tectonic and volcanic activities occurred in Southwestern Shandong Province, which significantly influenced the coals in this area [24,25]. The coals in Southwestern Shandong have been reported by many researchers, which have focused on the depositional environment [26,27], the tectonic–magmatic evolution [28,29], and trace-element geochemistry and mineralogical compositions [30–33]. However, no publications have elucidated the mineralogical anomalies, as well as their geological control in these coals. In some cases, magmatic intrusions can affect the safety, productivity, and economic viability of coal seams, and a few studies have investigated coals influenced by igneous intrusions, such as Fengfeng-Handan and Adaohai coals (both in North China) [34,35], as well as some coals from other areas over the world [36,37]. However, it is ambiguous as to whether hydrothermal fluids from magmatic activities have influenced the mineral assemblage in the Southwestern Shandong coals.

This paper presents the mineralogical compositions and characteristics in the No. 3 coal from the Jinyuan Mine, Tengxian coalfield. The aim was to analyze the mineral assemblages and occurrence modes in the No. 3 coal, all of which will further our understanding of the depositional environment and the mineralogical anomalies in the Jinyuan coals.

2. Geological Setting

The Tengxian coalfield is situated in southwest Shandong Province, eastern China (Figure 1), and covers an area of ~1398 km^2. The coalfield is divided into Tengbei Diggings (north area of the coalfield) and Tengnan Diggings (south area of the coalfield) based on Tengxian anticline (Figure 1). Abundant faults have been found in Tengnan Diggings, where the east, west and south sides are surrounded by the SN-Zeshan fault, SN-Sunshidian fault, and EW-Peicheng fault, respectively (Figure 1). The Tengnan Diggings also includes several coal mines, where the Jinyuan Mine, which is located in the southeast part of the Tengnan Diggings (Figure 1).

The major coal-bearing units in the Tengxian coalfield are the Pennsylvanian Taiyuan Formation and the Early Permian Shanxi Formation. The Taiyuan Formation is conformably overlying of the Benxi formation (Figure 2), which was deposited in a marine–terrestrial transitional environment and is represented by an average thickness of 180 m [38]. It is mainly comprised of mudstone, siltstone, limestone, fine grained sandstone, and coal seams. There are seven coal seams in this formation, while numbers 16 and 12 are minable, and numbers 17, 14 and 8 are partly minable coal seams [38] (Figure 2).

The Early Permian Shanxi Formation is an important coal-bearing stratum in this coalfield, having a thickness varying from 80–140 m, with an average thickness of 110 m [26]. The deposited environment of the bottom section of Shanxi Formation was a marine–terrestrial transitional environment, whereas the depositional environment was transformed to a continental sedimentary environment in the subsequent deposition processes. The lithological composition of the Shanxi Formation consists of fine–medium grained sandstone, siltstone, mudstone, sandy claystone and coal seams, where the No. 3 coal is the lowermost seam and is one of the dominating mineable coal seams of the Shanxi Formation in this area [26,38] (Figure 2). In the study area, the thickness of the No. 3 coal seam varies from 1.3 to 5.1 m (2.9 m on average). In some cases, the No. 3 coal seam is split into two different coal seams, namely No. 3S and No. 3X from top to bottom, both of which are minable coal seams.

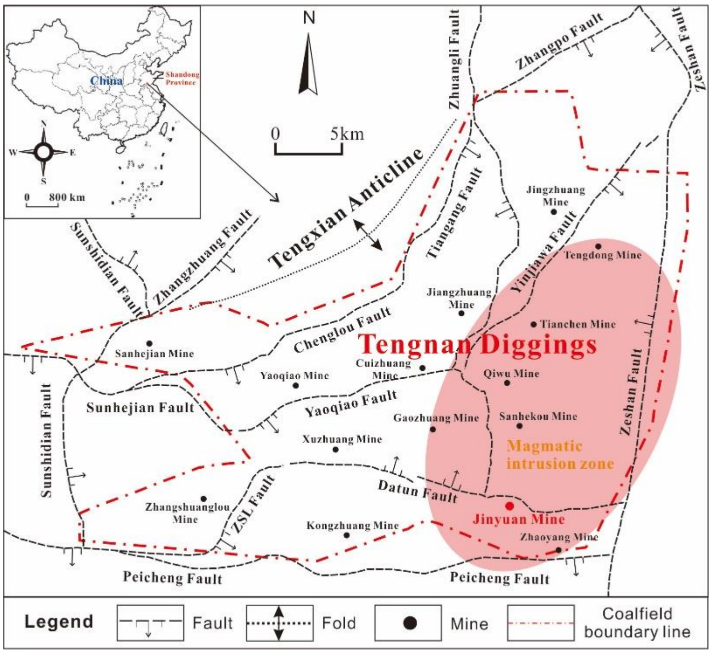

Figure 1. The geotectonic position of the Tengnan Diggings, as well as locations of coal mines and a geological map of Tengnan Diggings.

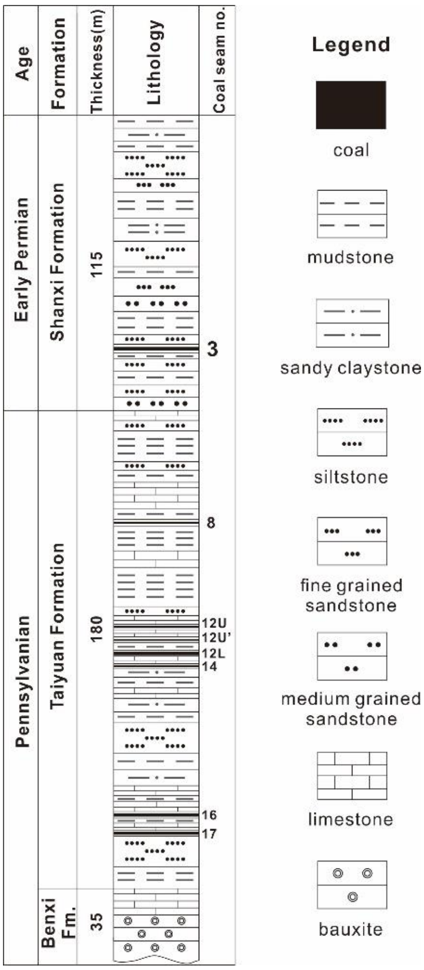

Figure 2. Stratigraphic section through the Tengxian coalfield, modified from Zhu [31].

During the later period of the Yanshan Movement (Cretaceous), frequent magmatic activities occurred in the Tengxian coalfield, especially in the Southeast of Tengnan Diggings, mainly distributed in the Zhaoyang, Jinyuan, Gaozhuang, Sanhekou, Qiwu and Tianchen coal mines (Figure 1). From south to north, magmatic activity weakens gradually [29]. The magmatic rocks in this area can be mainly divided into three types: lamprophyre, diorite, and diabase rocks [29].

3. Sample Collection and Analytical Methods

Eleven stratified samples, including 10 coal plies and associated one roof samples were taken from the upper portion of the No. 3 coal seam (JY-3) at the underground working face of the Jinyuan Mine, based on the Chinese Standard Method [39]. The lowermost portion of the No. 3 coal seam and associated floor samples are unavailable due to the limitations of coal mining craft and sample collection capacities. Coal bench samples were collected every 20 cm along the coal seam profile from top to bottom and identified as JY-3-R, JY-3-1c, JY-3-2c, JY-3-3c, JY-3-4c, JY-3-5c, JY-3-6c, JY-3-7c, JY-3-8c, JY-3-9c, and JY-3-10c. All collected samples were immediately wrapped with hop-pocket and sealed in plastic bags.

The coal ply samples were crushed and ground to <200-mesh for the proximate and mineralogical analyses. Proximate analysis was performed using the methods of American Society of Testing Materials (ASTM) Standards [40–44]. Mean random vitrinite reflectance was determined using An Axio Scope.A1 microscope equipped with a Craic 508 PV spectrophotometer based on ASTM Standard D2798-20 (2020) [45].

All coal ply samples were measured by oxygen–plasma ashing at a low temperature (EMITECH K1050X, 75 W Power, radio frequency system, <120 °C, Quorum Inc., Lewes, UK), and then the low temperature ashes were detected by X-ray diffraction analysis (XRD, Rigaku D/max-2200/PC, Tokyo, Japan). For the quantitative mineralogical analysis, all X-ray diffractograms were measured using a Siroquant^{TM} software (Sietronics Pty Ltd., Mitchell, Australia) developed by Taylor [46], and the detailed quantitative methods are published by a number of studies [47–53].

A scanning electron microscope (SU8200, JEOL, Tokyo, Japan) in conjunction with an energy-dispersive X-ray spectrometer (SU8200, Octane Super, AMETEK, Tokyo, Japan) at the Key Laboratory of Resource Exploration Research of Hebei Province were used to determine the distribution and modes of occurrence of minerals in polished specimen.

4. Results and Discussion

4.1. Coal Quality and Chemistry

Table 1 shows the results of proximate and related analyses such as, gross calorific value, total sulfur, and mean random vitrinite reflectance of the coal ply samples from the Jinyuan Mine. The results indicate that in addition to a few low to medium ash plies from the uppermost and lower part of the section, the majority of coal plies have low ash yields (<10%). Overall, the Jinyuan coal with an average ash yield of 11.35%, which is regarded as low-ash coal based on Chinese Standard GB/T 15224.1-2010 [54]. With the exception of samples JY-3-1c and JY-3-9c, which contain high total sulfur of 1.35% and 1.04%, respectively, other coal plies are characterized by low sulfur content (Table 1). Coal samples have an average of 0.44% total sulfur, corresponding to low-sulfur coal based on the classification by Chou [55].

Jinyuan coals are characterized by low moisture contents (1.34–1.74%, 1.54% on average) and high gross calorific values (30.76 MJ/kg on average). The volatile matter contents range from 33.32% to 47.71%, with an average of 38.95%. It should be noted that some lower-ash-yield coal plies (i.e., JY-3-2c, -4c, -7c) with highly volatile matter contents are caused by high contents of carbonate minerals, such as calcite. The mean random vitrinite reflectance is 0.76%. Therefore, the average vitrinite reflectance and values of volatile matter indicate that the Jinyuan coal is highly volatile A bituminous based on ASTM classification D388-12 (2012) [56].

Table 1. Proximate analysis (%), gross calorific values (MJ/kg), and mean random vitrinite reflectance values ($R_{o,ran}$; %) of the coal samples from the Jinyuan Mine.

Sample	M_{ad}	A_d	V_{daf}	$Q_{gr,d}$ (MJ/kg)	TS_d	$R_{o,ran}$
JY-3-1c	1.59	17.56	38.40	28.64	1.35	0.763
JY-3-2c	1.56	3.24	37.92	33.23	0.31	0.754
JY-3-3c	1.74	3.46	35.40	32.56	0.25	0.750
JY-3-4c	1.61	4.67	38.31	33.22	0.19	0.743
JY-3-5c	1.63	8.54	36.89	31.28	0.19	0.747
JY-3-6c	1.64	3.35	34.09	33.14	0.02	0.760
JY-3-7c	1.34	14.75	41.93	26.30	0.15	0.768
JY-3-8c	1.47	4.75	33.32	32.23	0.20	0.759
JY-3-9c	1.39	29.08	47.71	23.78	1.04	0.764
JY-3-10c	1.48	24.06	45.55	33.27	0.70	0.762
JY-3-Wa	1.54	11.35	38.95	30.76	0.44	0.757

ad, air-dried basis; d, dry basis; daf, ash-free basis; M, moisture; A, ash yield; V, volatile matter; TS, total sulfur; Q_{gr}, gross calorific value; $R_{o,ran}$, mean random vitrinite reflectance; W_a, weighted average.

4.2. Mineralogy

4.2.1. Minerals in the Jinyuan Coals

The composition of minerals in the Jinyuan No. 3 coal determined by powder XRD are presented in Table 2. The main minerals in the coal LTAs mainly consisted of kaolinite (56.0% on average), ankerite (10.8%), and illite (8.8%), and to a lesser extent, calcite (below detection limit (bdl)-54%, 7.8% on average), quartz (bdl-21.5%, 5.2% on average), and siderite (bdl-15.5%, 5.2% on average). In addition, traces of pyrite, jarosite, coquimbite, bassanite, rutile, and anatase were also found in several individual coal samples (Table 2).

Table 2. Contents of minerals of the Jinyuan coal LTAs and roof samples measured by XRD and Siroquant (%).

Sample	Kao	Illite	Qua	Cal	Ank	Plag	K-Feld	Sid	Py	Jaro	Coqu	Rut	Ana	Bass
JY-3-R	26.4	8.1	36.8			10.2	10.7	6.4	1.4					
JY-3-1c	42.7	17.3	21.5				0.5		5.3	11	1.4	0.3		
JY-3-2c	41.9	10	1.2		28.4			15.5	1.7					1.3
JY-3-3c	64.4	9.5	1.5	1.7	7.5			5				0.4	0.9	9
JY-3-4c	66	8.5	2.2	3.6	9.4			6.2				1	1.3	1.9
JY-3-5c	61.6	7.3	3	2.6	18.6			2.9				0.1	0.6	2.5
JY-3-6c	72.4	11.5		12.9				3.2						
JY-3-7c	11.4			54	34								0.6	
JY-3-8c	87.9		2.6		1.5			4.4				1.1	0.7	1.9
JY-3-9c	53	14.8	19.8						1.9	9.8	0.8			
JY-3-10c	59	9	0.5	3.6	8.1			14.4				0.7	0.8	3.9
JY-3-Wa	56.03	8.79	5.23	7.84	10.75			5.16	0.89	2.08	0.22	0.36	0.49	2.05

Kao, kaolinite; Qua, quartz; Cal, calcite; Ank, ankerite; Plag, plagioclase; K-Feld, K-Feldspar; Sid, siderite; Py, pyrite; Jaro, jarosite; Coqu; coquimbite; Rut, rutile; Ana, anatase; Bass, bassanite.

The minerals in the roof sample are predominantly quartz (36.8%), feldspar (plagioclase and k-feldspar, 20.9%), and kaolinite (26.4%), with a lower proportion of illite, siderite, and pyrite (Table 2).

Based on the mineral content and assemblage in each coal LTA sample (Table 2), three mineral assemblage types were observed in the No. 3 coals:

1. Type A is comprised of the samples JY-3-1c and JY-3-9c, with relatively high ash yields, quartz, pyrite, and sulfate minerals (i.e., jarosite and coquimbite), while carbonate minerals (i.e., calcite, ankerite, and siderite) were not detected by XRD. The sample JY-3-1c is located in the uppermost coal section, where the JY-3-9c sample is close to the bottom of the seam.

2. Type B consists of the samples of JY-3-2c, JY-3-3c, JY-3-4c, JY-3-5c, JY-3-6c, JY-3-8c, and JY-3-10c, with low contents of ash yield and quartz, however, various contents of carbonate minerals (calcite, ankerite, and siderite) occurred in this Type. Pyrite and sulfate minerals (jarosite and coquimbite) were rare in these coal samples. In addition, these samples mainly occurred in the middle part of the coal seam.
3. Only sample JY-3-7c belongs to Type C, which contains a high proportion of calcite (54%) and ankerite (or dolomite, 34%), and, to a lesser extent, kaolinite (11.4%).

4.2.2. Modes of Mineral Occurrence

The X-ray diffractograms display that the poorly ordered kaolinite is found in the Type A, while kaolinite in the Type B samples is well ordered (Figure 3). Permana et al. [57] and Wang et al. [33] have reported a similar phenomenon in some coals from the Bowen Basin and the Southwestern Shandong coalfields, respectively, and the latter is adjacent to the coals in this study. Kaolinite was observed to occur as cell-fillings (Figure 4A), matrix intimately mixed with detrital quartz (Figure 4B), and pelletoidal fine particles (1–5 μm, Figure 4C) under the optical and SEM. Kaolinite with the former two forms mainly occured in samples from Type A. In most cases, the pelletoidal fine particles of kaolinite are distributed along bedding planes, or alternatively, assembled as irregular to ellipsoidal aggregates. This form of kaolinite is common in samples from Type B, in addition, XRD patterns show the structure of the kaolinite is well ordered in these samples, and this probably indicates that pelletoidal fine kaolinite particles are of terrigenous origin, while kaolinite is carried into (washed or blown) and preserved in the peat deposit, and subsequent diagenesis would lead to the increase in the structural order of kaolinite [58]. Trace amounts of kaolinite occur as fracture-fillings (Figure 4D), indicating an epigenetic precipitation.

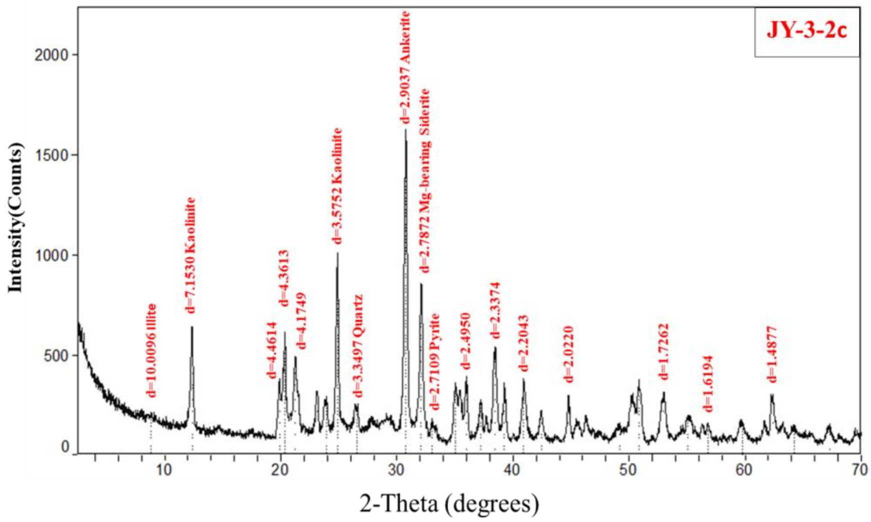

Figure 3. Identification of the well-ordered structure of kaolinite and siderite (contains Mg) in the X-ray diffractogram of sample JY-3-2c.

Illite present in the Jinyuan coal was mainly found to be in layers along the bedding planes (Figure 4E,F), suggesting a detrital origin. The cell-filling paragonite (($NaAl_2(AlSi_3)O_{10}(OH)_2$)), which was observed in few coal plies by SEM, occurs as cell-fillings, indicating an authigenic origin (Figure 5A). In a few cases, paragonite also co-exists with kaolinite (Figure 5B–D).

Quartz in the No. 3 coals occurs in three forms: (1) as scattered irregular grains distributed in clay matrix or organic matter, with a size commonly more than 10 μm (Figure 4B; Figure 6A,B), indicating a detrital origin; (2) as cell-fillings (Figure 6B) and (3) as discrete fine particles (<10 μm) embedded in collodetrinite (Figure 6C,D). Quartz with the latter two forms suggests an authigenic origin.

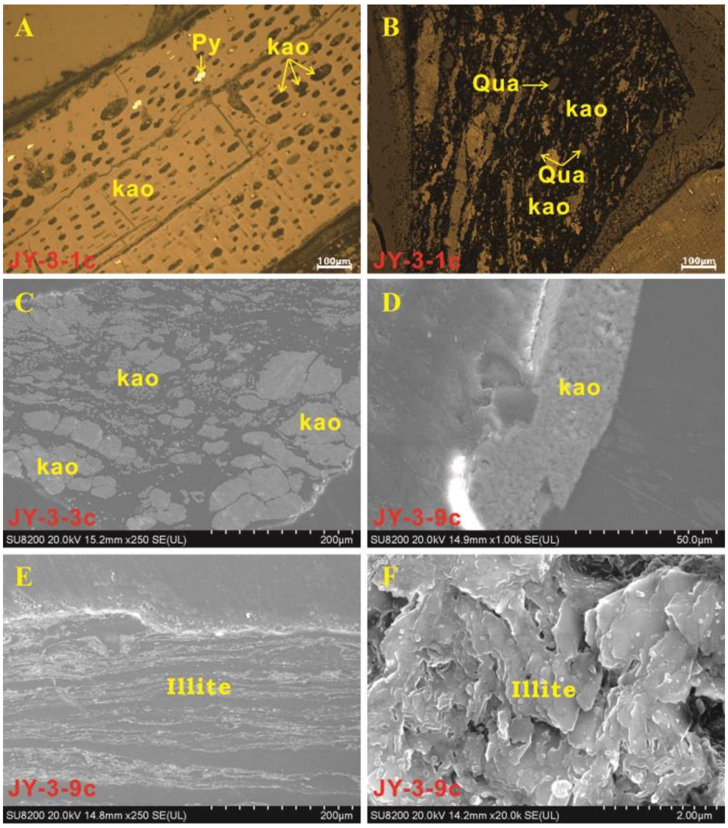

Figure 4. Reflected light optical microscope and SEM secondary electronic images of minerals in the Jinyuan Coal. (**A**), cell-filling kaolinite (Kao) and Pyrite (Py); (**B**), kaolinite distributed along bedding planes; (**C**), kaolinite occurring as pelletoidal fine particles; (**D**), fracture-filling kaolinite; (**E**,**F**), Illite distributed along bedding planes.

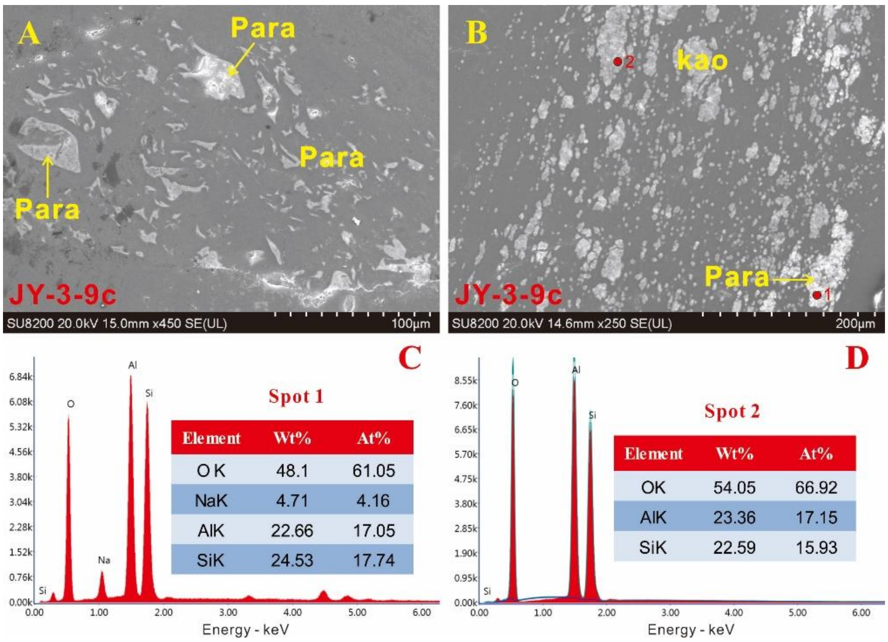

Figure 5. SEM secondary electronic images of paragonite (Para) and kaolinite (Kao) in sample JY-3-9c. (**A**), cell-filling paragonite; (**B**), paragonite co-existing with kaolinite; (**C**,**D**) are EDS spectrums of respective test spots in (**B**).

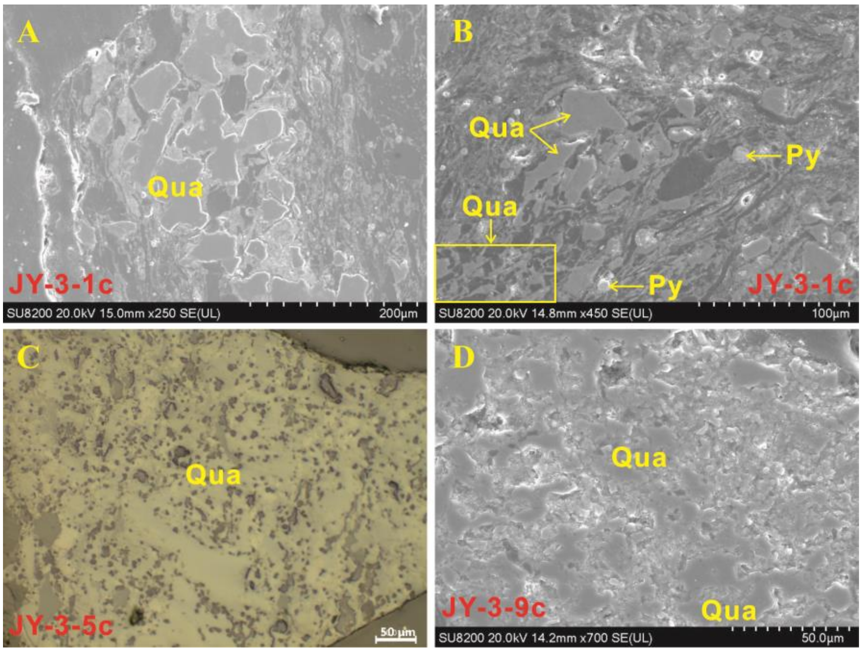

Figure 6. SEM secondary electronic and reflected light optical microscope images of Quartz (Qua) in the JY-3 Coal. (**A**,**B**), detrital quartz and cell-filling quartz; (**C**,**D**), authigenic quartz.

Ankerite, calcite and siderite are the dominated carbonate minerals in the No. 3 coals. The X-ray diffractogram shows that the siderite in the coal is characterized by a basal peak at 2.787 Å, which is relatively low compared to the normal siderite (2.795 Å) (Figure 3). It is thus probably identified as Mg-bearing siderite [59]. In addition, SEM-EDS study also shows that it contains a trace of Mg (Figure 7F). Under the SEM, ankerite and calcite are mainly present as fusinite-cell-fillings (Figure 7A,B) and vein-fillings (Figure 7C,D), indicating an epigenetic origin [60]. Mg-bearing siderite has similar modes of occurrence to ankerite and calcite, generally occuring in fracture-fillings (Figure 7E), suggesting that its formation is of hydrothermal origin as well.

Pyrite was mainly detected in samples from Type A and has various modes of occurrence. It occurs as isolated or clustered framboids (Figure 8A,B), as well as subhedral to euhedral crystals (Figure 8B,C), cell-fillings (Figure 8D), and massive forms in the clay minerals matrix (Figure 8E), which probably indicate syngenetic, or early diagenetic origin [8,55,61,62]. To a lesser extent, the fracture-filling pyrite, which indicates an epigenetic precipitation of hydrothermal solutions [63,64], was also observed under the SEM (Figure 8F).

Sulphate minerals in the coals include jarosite and coquimbite, which were detected only in samples from Type A that were enriched in higher pyrite concentrations than others coal plies. Some framboidal pyrites are corroded and replaced by jarosite (Figure 8G,H), and in some cases, the outside edge of the corroded pyrite is substituted by jarosite as well (Figure 8I). Such modes of occurrence of the jarosite may represent an oxidation product of pyrite [8,65,66].

A small proportion of bassanite was determined by XRD analysis in several of the Jinyuan LTAs, especially those plies from Type B which have low ash yields; however, it is absent in the floor sample and samples from Type A. In some cases, the bassanite could have formed by dehydration of gypsum, while gypsum was formed by the interaction between the sulphuric acid and the Ca, which is derived from the oxidation of pyrite and released from calcite, respectively [7,67–70]. However, bassanite in this study is not relevant to jarosite, as well as other minerals formed by pyrite oxidation, hence, the formation of bassanite is more likely due to the interaction between organically-associated sulphur and calcium during the plasma-ashing process [7,65,71–73].

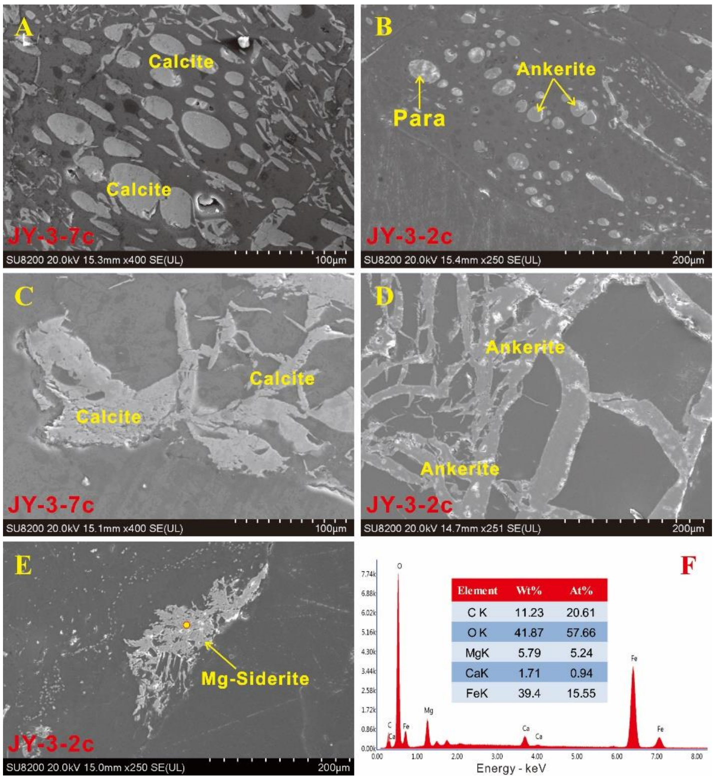

Figure 7. SEM secondary electronic images and EDS spectra of carbonate minerals in the JY-3 Coal. (**A**,**B**), cell-filling calcite, ankerite and paragonite (Para); (**C**,**D**), epigenetic calcite and ankerite; (**E**), Mg-bearing siderite; (**F**), EDS spectra of spot in (**E**).

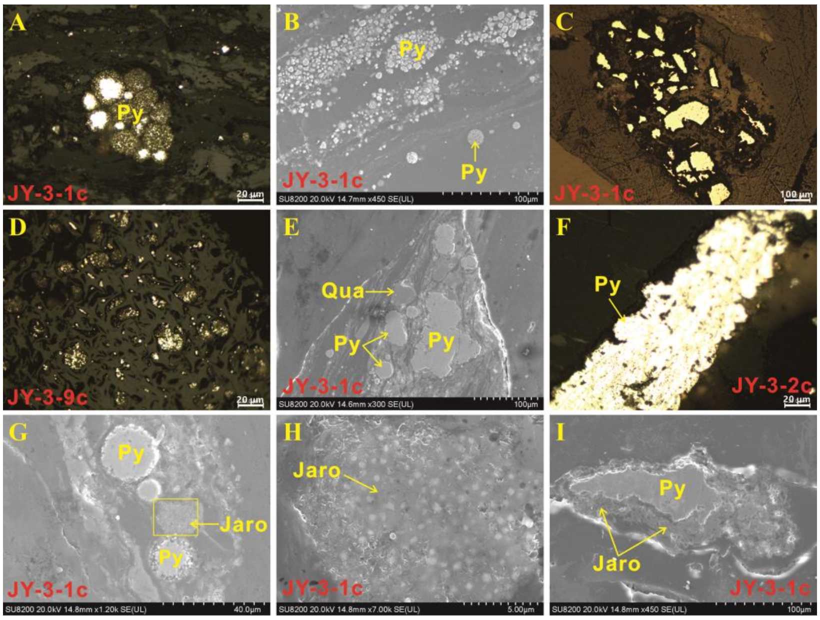

Figure 8. Reflected light optical microscope and SEM secondary electronic images of Pyrite (Py) and jarosite (Jaro) in the Jinyuan Coal. (**A**–**C**), pyrite framboids and subhedral to euhedral crystals pyrite; (**D**), cell-filling pyrite; (**E**), massive pyrite; (**F**), fracture-filling pyrite; (**G**–**I**), jarosite, (**H**) is the enlargement of rectangle in (**G**).

Trace amounts of anatase or rutile are also detected in some coal plies by using XRD. Anatase in the coals primarily occurs as scattered particles in organic matter (Figure 9A). Albite and K-feldspar in the Jinyuan coal occur as discrete, irregular, angular particles distributed in the clay matrix (Figure 9B). The similar morphology of the anatase and feldspars indicate that both have detrital origins [66,74].

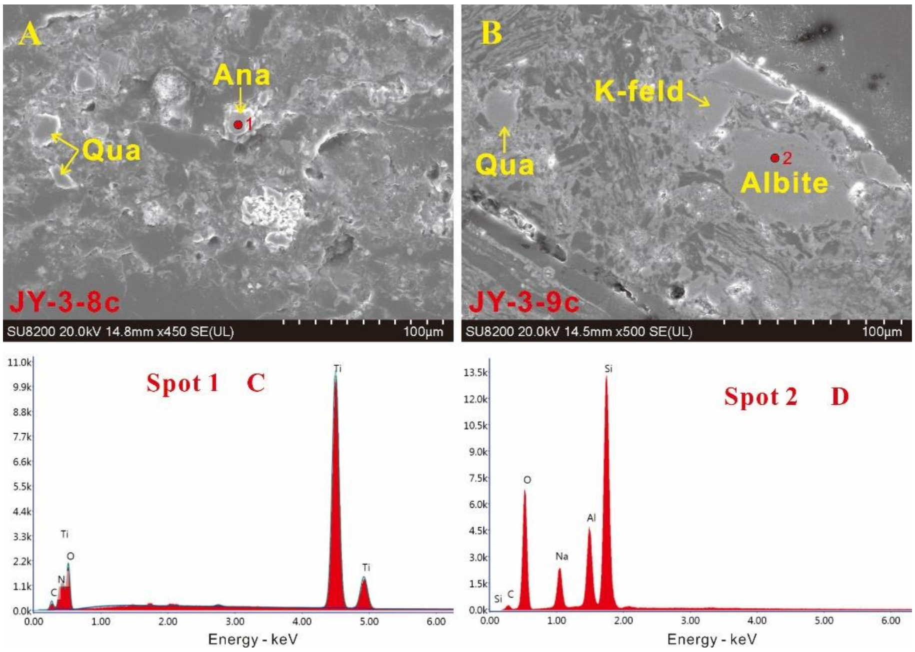

Figure 9. SEM secondary electronic images of anatase (Ana), K-feldspars (K-feld) and albite in the JY-3 Coal. (**A**,**B**), detrital anatase and feldspars; (**C**,**D**) are EDS spectrums of respective test spots in (**A**,**B**).

4.3. Discussion: Origin of Minerals in the Jinyuan Coals

The minerals in the No. 3 coals from the Jinyuan Mine are of terrigenous, authigenic, and epigenetic origin. Three factors have been identified that affect coal mineralogical anomalies and modes of occurrence in the Jinyuan coals, including detrital input, multi-stage hydrothermal activities, and seawater influence.

4.3.1. Detrital Input

As mentioned above, the occurrence modes of quartz, poorly ordered kaolinite, illite, and the trace of feldspars and anatase in the Jinyuan coals, occurring as scattered particles, as well as layers along the bedding planes, indicate that they were terrigenous detrital minerals. These detrital minerals were found in the bench close to the roof or the bottom of the seam, which typically have relatively high ash yields, suggesting greater amounts of terrigenous materials influx into the accumulating peat deposit [8,75]. However, such detrital minerals are rare in the low-ash yield samples which are in the middle of the coal seam profile, where the kaolinite is abundant and mainly occurs as pelletoidal fine kaolinite (as described above). This may be due to the vegetation in or around the peat mire, which serves as a natural barrier, restraining detrital minerals, especially large quartz and feldspar particles, from penetrating into the peat swamp [6,7], however, kaolinite is fine in size, thus, it can effectively migrate into and be deposited in the peat mire [33]. Oppositely, during the formation of the uppermost coal section, the intensity of tectonic movement was increased, which affects the vegetation growth and weakens the prevention of vegetation at the same time [33], thus allowing detrital minerals to be preserved in the uppermost coal ply [33,51]. Thus, the input of the detrital minerals is one of the most prominent factors that control ash yields and mineral assemblages in the coals studied.

4.3.2. Multi-Stage Hydrothermal Activities

In addition to the input of the detrital minerals, multi-stage hydrothermal fluids also play a critical role in influencing the mineral anomalies in the Jinyuan coals.

Based on the modes of occurrence of minerals, kaolinite and pyrite occur as cell-fillings, suggesting an authigenic origin, these mineral phases more likely formed by the invasion of syngenetic hydrothermal fluids to the coal seam. The mode of occurrence of paragonite implies its authigenic origin rather than terrigenous origin. Although uncommon in coal seams, paragonite is relatively widespread in low-grade metamorphic rocks [76,77] and high rank anthracites [78–80], in some cases, paragonite has been found in low-rank coal areas affected by heat-induced metamorphism [65]. Wang et al. [59] noted that paragonite in the Late Permian coals from the Changxing Mine (Southwestern China) was probably a product of the dissolution and recrystallization of mixed-layer I/S during coal metamorphism. Susilawati and Ward [65] suggested that the paragonite in the coal from the Bukit Asam deposit, South Sumatra, was derived from the interaction between kaolinite and Na-bearing hydrothermal fluids. Although paragonite mostly occurs in higher rank coals, it also occurs in high-volatile bituminous Permian coal from the Sydney Basin, Australia [75]. In this study, paragonite in the No.3 coals mainly occurs as cell-fillings and co-exists with kaolinite, suggesting that paragonite in Jinyuan coals may have been derived from the precipitated by the Na-rich fluids. However, the source of Na-rich fluids warrants further investigation.

Authigenic quartz was probably syngenetically precipitated from the silicious solutions. A similar phenomenon was discovered in many Southwestern Chinese coals, such as the Xuanwei coals [81] and the Yueliangtian coals [82,83].

Epigenetic vein-like calcite, ankerite, and siderite are widely found in Jinyuan coals, especially abundant in sample JY-3-7c, which has high contents of calcite (54%) and ankerite (34%). In general, the acidic environment of normally peat-swamp is not conducive to the existence of carbonate minerals [33,73,84,85]. In most instances, the epigenetic carbonate minerals can be precipitated either from Ca (Mg, Fe)-bearing meteoric fluids or underground water during the coal-formation process. However, many scholars reported a great abundance of cleat- or fracture-fillings carbonate minerals in these coals adjacent to igneous intrusions, which are derived from hydrothermal alteration of the igneous material [86–89]. A previous study by Dai et al. [35] has noticed that high contents of calcite and dolomite in the Adaohai coals were derived from igneous fluids. However, Dai et al. [89,90] reported carbonate minerals in the Guanbanwusu and Haerwusu coals as well, located adjacent to the Adaohai coal which were not derived from igneous intrusions, because the rank of these coals are distinctly lower than the Adaohai coal. Similarly, in the present study, although frequent magmatic activity occurred in the research area during the later period of the Yanshan Movement, it appears that the carbonate minerals were not derived from igneous intrusions, because the volatile matter yield and the rank of the Jinyuan coal are close to the contemporaneous Luxi, Liangbaosi, and Tangkou coals from the adjacent coalfields [33]. Furthermore, although epigenetic vein-like carbonate minerals are abundant in sample JY-3-9c, as well as the occurrence of paragonite in this sample, the vitrinite reflectance of this sample has no obvious change compared to other coal plies, possibly indicating that the Jinyuan coal does not seem to be influenced by the apparent intrusion of magma. Therefore, the formation temperature of these epigenetic minerals such as calcite and paragonite was not too high [89].

In addition, the cell-filling calcite, fracture-filling kaolinite, and fracture-filling pyrite observed in the study coals are also due to the influx of hydrothermal fluids influx during different periods of the coal formation.

4.3.3. Seawater Influence

Previous studies have indicated that the peat depositional environment of the Shanxi Formation in the study area was the marine–terrestrial transitional environment at the early stage [38]. In the present study, the No. 3 coal belongs to the lower part of the Shanxi Formation, which was deposited in a lagoon environment in the Tengnan coalfield [26], in addition, studies by Chen et al. [91] have also shown that seawater affected the bottom section of the Shanxi Formation.

High concentrations of sulfur and the presence of syngenetic pyrite in coals are used to indicate a depositional environment under the influence of seawater by many scholars [11,33,55]. Chou [55] noticed that the sulfur in low sulfur coal (<1%, total sulfur) is derived mainly from parent plant material. In the present study, the sulfur concentration varies from 0.02% to 1.35%, the average sulfur content is lower than 1%, however, it should be mentioned that a relatively high sulfur content has been found in some coal plies, especially in the uppermost coal section (JY-3-1c, 1.35%). In addition, the morphology characteristics of pyrite are framboids, euhedral crystals, and massive form that observed in these high sulfur content samples, indicating a syngenetic origin. Hence, some high-sulfur coal samples in the No. 3 coal are more likely to be affected by intermittent seawater influence during peat forming. Previous studies on contemporaneous coals from the adjacent three coalfields (Southwestern Shandong), with the same content and distribution characteristics of sulfur, also support that the seawater intrusion occurred on a large scale during this period [33].

5. Conclusions

The Early Permian coal from the Jinyuan Mine in Shandong Province, Eastern China is a highly volatile A bituminous coal, with low-ash and low-sulfur contents. Minerals identified in the Jinyuan coals mainly represented by kaolinite, ankerite, illite, calcite, siderite, quartz, and trace amounts of pyrite, jarosite, bassanite, anatase, and rutile. The kaolinite, quartz, and illite were derived from terrigenous materials during peat accumulation. The formation of syngenetic pyrite is generally induced by seawater, while the sulphate minerals (jarosite and coquimbite) were produced by pyrite oxidation. The modes of occurrence of carbonate minerals indicate they were formed by the precipitation of the Ca, Mg, or Fe-bearing fluids. The paragonite in the coal is probably precipitated from Na-rich fluids, while the origin of this Na-rich hydrothermal warrants further investigation. Effects of magmatic intrusion on mineralogy were not investigated in this paper, in addition, the formation temperatures associated with the carbonate minerals were not high enough to raise the vitrinite reflectance.

Author Contributions: W.G.: Conceptualization, Writing-Original draft preparation. J.L.: Formal analysis, Data curation. Z.W.: Formal analysis, Data curation. K.Z.: Formal analysis, Data curation. Z.G.: Formal analysis, Data curation. J.M.: Writing-Reviewing and Editing, Supervision. C.Z.: Writing-Reviewing and Editing, Supervision. All authors have read and agreed to the published version of the manuscript.

Funding: This research was supported by the National Natural Science Foundation of China (No. 41872173), the Science Foundation of Hebei (No. 2016402104). The authors sincerely thank Dr. Bangjun Liu for the assistance of language polishing.

Acknowledgments: The authors sincerely thank Bangjun Liu for the assistance of language polishing.

Conflicts of Interest: The authors declare no conflict of interest.

References

1. Thurber, M.C.; Morse, R.K. *The Global Coal Market: Supplying Major Fuel for Emerging Economies*; Cambridge University Press: Cambridge, UK, 2015; p. 702.
2. World Coal Association. 2019. Available online: https://www.worldcoal.org/coal (accessed on 6 January 2019).
3. BP Statistical Review of World Energy. *BP Statistical Review of World Energy*; BP Statistical Review of World Energy: London, UK, 2019; Available online: http://www.bp.com/statisticalreview (accessed on 5 August 2020).
4. Dai, S.; Finkelman, R.B. Coal geology in China: An overview. *Int. Geol. Rev.* **2018**, *60*, 531–534. [CrossRef]
5. Finkelman, R.B. Trace and minor elements in coal. In *Organic Geochemistry*; Engel, M.H., Macko, S.A., Eds.; Springer: Boston, MA, USA, 1993; pp. 593–607.
6. Saxby, J.D. Minerals in coal. In *Organic Matter and Mineralisation: Thermal Alteration, Hydrocarbon Generation and Role in Metallogenesis*; Springer: Berlin, Germany, 2000; pp. 314–328.
7. Ward, C.R. Analysis and significance of mineral matter in coal seams. *Int. J. Coal Geol.* **2002**, *50*, 135–168. [CrossRef]

8. Ward, C.R. Analysis, origin and significance of mineral matter in coal: An updated review. *Int. J. Coal Geol.* **2016**, *165*, 1–27. [CrossRef]
9. Ren, D.; Zhao, F.; Wang, Y.; Yang, S. Distributions of minor and trace elements in Chinese coals. *Int. J. Coal Geol.* **1999**, *40*, 109–118. [CrossRef]
10. Finkelman, R.B.; Palmer, C.A.; Wang, P. Quantification of the modes of occurrence of 42 elements in coal. *Int. J. Coal Geol.* **2018**, *185*, 138–160. [CrossRef]
11. Dai, S.; Bechtel, A.; Eble, C.F.; Flores, R.M.; French, D.; Graham, I.T.; Hood, M.M.; Hower, J.C.; Korasidis, V.A.; Moore, T.A.; et al. Recognition of peat depositional environments in coal: A review. *Int. J. Coal Geol.* **2020**, *219*, 103383. [CrossRef]
12. Finkelman, R.B. Modes of occurrence of potentially hazardous elements in coal: Levels of confidence. *Fuel Process. Technol.* **1994**, *39*, 21–34. [CrossRef]
13. Clemens, A.H.; Deely, J.M.; Gong, D.; Moore, T.A.; Shearer, J.C. Trace element partitioning behavior during coal combustion–the influence of events occurring during the deposition stage. *Fuel* **2000**, *79*, 1781–1784. [CrossRef]
14. Finkelman, R.B.; Dai, S.; French, D. The importance of minerals in coal as the hosts of chemical elements: A review. *Int. J. Coal Geol.* **2019**, *212*, 103251. [CrossRef]
15. Chou, C.-L. Geological factors affecting the abundance, distribution, and speciation of sulfur in coals. In *Geology of Fossil Fuels-Coal, Proceedings of the 30th International Geological Congress*; Yang, Q., Ed.; VSP: Utrecht, The Netherlands, 1997; Volume 18, pp. 47–57.
16. Zheng, B.; Ding, Z.; Huang, R.; Zhu, J.; Yu, X.; Wang, A.; Zhou, D.; Mao, D.; Su, H. Issues of health and disease relating to coal use in southwest China. *Int. J. Coal Geol.* **1999**, *40*, 119–132. [CrossRef]
17. Ding, Z.; Zheng, B.; Long, J.; Belkin, H.E.; Finkelman, R.; Chen, C.; Zhou, D.; Zhou, Y. Geological and geochemical characteristics of high arsenic coals from endemic arsenosis areas in southwestern Guizhou Province, China. *Appl. Geochem.* **2001**, *16*, 1353–1360. [CrossRef]
18. Finkelman, R.B.; Orem, W.; Castranova, V.; Tatu, C.A.; Belkin, H.E.; Zheng, B.; Lerch, H.E.; Maharaj, S.V.; Bates, A.L. Health impacts of coal and coal use: Possible solutions. *Int. J. Coal Geol.* **2002**, *50*, 425–443. [CrossRef]
19. Dai, S.; Ren, D.; Ma, S. The cause of endemic fluorosis in western Guizhou Province, Southwest China. *Fuel* **2004**, *83*, 2095–2098. [CrossRef]
20. Dai, S.; Ren, D.; Tang, Y.; Yue, M.; Hao, L. Concentration and distribution of elements in Late Permian coals from western Guizhou Province, China. *Int. J. Coal Geol.* **2005**, *61*, 119–137. [CrossRef]
21. Dai, S.; Ren, D.; Chou, C.-L.; Finkelman, R.B.; Seredin, V.V.; Zhou, Y. Geochemistry of trace elements in Chinese coals: A review of abundances, genetic types, impacts on human health, and industrial utilization. *Int. J. Coal Geol.* **2012**, *94*, 3–21. [CrossRef]
22. Finkelman, R.B.; Tian, L. The health impacts of coal use in China. *Int. Geol. Rev.* **2017**, *60*, 579–589. [CrossRef]
23. Zhao, L.; Dai, S.; Finkelman, R.B.; French, D.; Graham, I.T.; Yang, Y.; Li, J.; Yang, P. Leaching behavior of trace elements from fly ashes of five Chinese coal power plants. *Int. J. Coal Geol.* **2020**, *219*, 103381. [CrossRef]
24. Li, W. Workflows of identification of the coalfield tectonic types. *Coal Geol. China* **1998**, *10*, 4–9.
25. Li, X.; Li, S.; Suo, Y.; Somerville, I.D.; Huang, F.; Liu, X.; Wang, P.; Han, Z.; Jin, L. Early Cretaceous diabases, lamprophyres and andesites-dacites in western Shandong, North China Craton: Implications for local delamination and Paleo-Pacific slab rollback. *J. Asian Earth Sci.* **2018**, *160*, 426–444. [CrossRef]
26. Xue, Q. Depositional architectures and coal-forming features of shallow-water delta system in the Tengnan coal mine district, Shandong Province. *J. China Univ. Mingin Technol.* **1995**, *24*, 43–51, (In Chinese with English abstract).
27. Han, M.; Wei, J. Deltaic depositional system and coal-accumulation in Juye Coalfield. *Acta Sedimentol. Sin.* **2001**, *19*, 381–385, (In Chinese with English abstract).
28. Wang, Y. Carboniferous-Permian pyroclastic rocks in Jining, Juye and Tengxian coalfields. *Coal Geol. Explor.* **1990**, *4*, 9–12. (In Chinese)
29. Tang, D.; Bie, L.; Mi, J.; Pan, W. Magma intrusion feature and its influence to coal seam in Tengnan mining field. *J. Min. Saf. Eng.* **2003**, *20*, 109–111. (In Chinese)
30. Zeng, R.; Zhuang, X.; Yang, S. Quality of the coals from middle area of coal-bearing district of western Shandong. *Coal Geol China* **2000**, *12*, 10–15.

31. Liu, G.; Zheng, L.; Gao, L.; Zhang, H.; Peng, Z. The characterization of coal quality from the Jining coalfield. *Energy* **2005**, *30*, 1903–1914. [CrossRef]
32. Liu, G.; Zheng, L.; Zhang, Y.; Qi, C.; Chen, Y.; Peng, Z. Distribution and mode of occurrence of As, Hg and Se and sulfur in coal Seam 3 of the Shanxi Formation, Yanzhou coalfield, China. *Int. J. Coal Geol.* **2007**, *71*, 371–385. [CrossRef]
33. Wang, X.; Zhang, L.; Jiang, Y.; Chen, Z. Mineralogical and Geochemical Characteristics of the Early Permian Upper No. 3 Coal from Southwestern Shandong, China. *Minerals* **2016**, *6*, 58. [CrossRef]
34. Dai, S.; Ren, D. Effects of magmatic intrusion on mineralogy and geochemistry of coals from the Fengfeng-Handan Coalfield, Hebei, China. *Energy Fuels* **2007**, *21*, 1663–1673. [CrossRef]
35. Dai, S.; Zou, J.; Jiang, Y.; Ward, C.R.; Wang, X.; Li, T.; Xue, W.; Liu, S.; Tian, H.; Sun, X.; et al. Mineralogical and geochemical compositions of the Pennsylvanian coal in the Adaohai Mine, Daqingshan Coalfield, Inner Mongolia, China: Modes of occurrence and origin of diaspore, gorceixite, and ammonian illite. *Int. J. Coal Geol.* **2012**, *94*, 250–270. [CrossRef]
36. Li, K.; Rimmer, S.M.; Presswood, S.M.; Liu, Q. Raman spectroscopy of intruded coals from the Illinois Basin: Correlationwith rank and estimated alteration temperature. *Int. J. Coal Geol.* **2020**, *219*, 103369. [CrossRef]
37. Sanders, M.M.; Rimmer, S.M. Revisiting the thermally metamorphosed coals of the Transantarctic Mountains, Antarctica. *Int. J. Coal Geol.* **2020**, *228*, 103550. [CrossRef]
38. Zhu, Y. The Biotic Types and Stratigraphic Subdivision of Late Paleozoic Age in Tengxian Coalfield of Shandong-on Carboniferous-Permian Boundary. Master's Thesis, Shandong University of Science and Technology, Shandong, China, 2006. (In Chinese).
39. Coal Analysis Laboratory of China Coal Research Institute. *Chinese Standard Method GB/T 482-2008, Sampling of Coal Seams*; National Coal Standardization Technical Committee: Beijing, China, 2008.
40. ASTM International. *Test Method for Ash in the Analysis Sample of Coal and Coke*; ASTM D3174-11; ASTM International: West Conshohocken, PA, USA, 2011.
41. ASTM International. *Test Method for Moisture in the Analysis Sample of Coal and Coke*; ASTM D3173-11; ASTM International: West Conshohocken, PA, USA, 2011.
42. ASTM International. *Test Method for Volatile Matter in the Analysis Sample of Coal and Coke*; ASTM D3175-11; ASTM International: West Conshohocken, PA, USA, 2011.
43. ASTM International. *Test Method for Gross Calorific Value of Coal and Coke*; ASTM D5865-13; ASTM International: West Conshohocken, PA, USA, 2013.
44. ASTM International. *Test Methods for Total Sulfur in the Analysis Sample of Coal and Coke*; ASTM D3177-02; ASTM International: West Conshohocken, PA, USA, 2002.
45. ASTM International. *Test Method for Microscopical Determination of the Vitrinite Reflectance of Coal*; ASTM D2798-20; ASTM International: West Conshohocken, PA, USA, 2020.
46. Taylor, J.C. Computer programs for standard less quantitative analysis of minerals using the full powder diffraction profile. *Powder Diffr.* **1991**, *6*, 2–9. [CrossRef]
47. Rietveld, H.M. A profile refinement method for nuclear and magnetic structures. *J. Appl. Crystallogr.* **1969**, *2*, 65–71. [CrossRef]
48. Ward, C.R.; Taylor, J.C.; Matulis, C.; Dale, L. Quantification of mineral matter in the Argonne Premium Coals using interactive Rietveld-based X-ray diffraction. *Int. J. Coal Geol.* **2001**, *46*, 67–82. [CrossRef]
49. Ruan, C.-D.; Ward, C.R. Quantitative X-ray powder diffraction analysis of clay minerals in Australian coals using Rietveld methods. *Appl. Clay Sci.* **2002**, *21*, 227–240. [CrossRef]
50. Zhao, L.; Ward, C.R.; French, D.; Graham, I.T.; Dai, S.; Yang, C.; Xie, P.; Zhang, S. Origin of a kaolinite-NH 4 -illite-pyrophyllite-chlorite assemblage in a marine-influenced anthracite and associated strata from the Jincheng Coalfield, Qinshui Basin, Northern China. *Int. J. Coal Geol.* **2018**, *185*, 61–78. [CrossRef]
51. Spiro, B.F.; Liu, J.; Dai, S.; Zeng, R.; Large, D.; French, D. Marine derived 87Sr/86Sr in coal, a new key to geochronology and palaeoenvironment: Elucidation of the India-Eurasia and China-Indochina collisions in Yunnan, China. *Int. J. Coal Geol.* **2019**, *215*, 103304. [CrossRef]
52. Liu, J.; Song, H.; Dai, S.; Nechaev, V.P.; Graham, I.T.; French, D.; Nechaeva, E.V. Mineralization of REE-Y-Nb-Ta-Zr-Hf in Wuchiapingian coals from the Liupanshui Coalfield, Guizhou, southwestern China: Geochemical evidence for terrigenous input. *Ore Geol. Rev.* **2019**, *115*, 103190. [CrossRef]

53. Liu, J.; Nechaev, V.P.; Dai, S.; Song, H.; Nechaeva, E.V.; Jiang, Y.; Graham, I.T.; French, D.; Yang, P.; Hower, J.C. Evidence for multiple sources for inorganic components in the Tucheng coal deposit, western Guizhou, China and the lack of critical-elements. *Int. J. Coal Geol.* **2020**, *223*, 103468. [CrossRef]
54. Coal Analysis Laboratory of China Coal Research Institute. *Chinese Standard Method GB/T 15224.1-2010, Classification for Quality of Coal. Part 1: Ash*; Standardization Administration of China: Beijing, China, 2010. (In Chinese)
55. Chou, C.-L. Sulfur in coals: A review of geochemistry and origins. *Int. J. Coal Geol.* **2012**, *100*, 1–13. [CrossRef]
56. ASTM International. *Standard Classification of Coals by Rank*; ASTM D388-12; ASTM International: West Conshohocken, PA, USA, 2012.
57. Permana, A.K.; Ward, C.R.; Li, Z.; Gurba, L.W. Distribution and origin of minerals in high-rank coals of the South Walker Creek area, Bowen Basin, Australia. *Int. J. Coal Geol.* **2013**, *116*, 185–207. [CrossRef]
58. Zhao, L.; Ward, C.R.; French, D.; Graham, I.T. Mineralogical composition of Late Permian coal seams in the Songzao Coalfield, southwestern China. *Int. J. Coal Geol.* **2013**, 208–226. [CrossRef]
59. Wang, X.; Zhang, M.; Zhang, W.; Wang, J.; Zhou, Y.; Song, X.; Li, T.; Li, X.; Liu, H.; Zhao, L. Occurrence and origins of minerals in mixed-layer illite/smectite-rich coals of the Late Permian age from the Changxing Mine, eastern Yunnan, China. *Int. J. Coal Geol.* **2012**, *102*, 26–34. [CrossRef]
60. Dai, S.; Chou, C.-L.; Yue, M.; Luo, K.; Ren, D. Mineralogy and geochemistry of a Late Permian coal in the Dafang Coalfield, Guizhou, China: Influence from siliceous and iron-rich calcic hydrothermal fluids. *Int. J. Coal Geol.* **2005**, *61*, 241–258. [CrossRef]
61. Dai, S.; Ren, D.; Tang, Y.; Shao, L.; Li, S. Distribution, isotopic variation and origin of sulfur in coals in the Wuda coalfield, Inner Mongolia, China. *Int. J. Coal Geol.* **2002**, *51*, 237–250. [CrossRef]
62. Dai, S.; Seredin, V.V.; Ward, C.R.; Hower, J.C.; Xing, Y.; Zhang, W.; Song, W.; Wang, P. Enrichment of U–Se–Mo–Re–V in coals preserved within marine carbonate successions: Geochemical and mineralogical data from the Late Permian Guiding Coalfield, Guizhou, China. *Miner. Depos.* **2014**, *50*, 159–186. [CrossRef]
63. Dai, S.; Yang, J.; Ward, C.R.; Hower, J.C.; Liu, H.; Garrison, T.M.; French, D.; O'Keefe, J.M.K. Geochemical and mineralogical evidence for a coal-hosted uraniumdeposit in the Yili Basin, Xinjiang, northwestern China. *Ore Geol. Rev.* **2015**, *70*, 1–30. [CrossRef]
64. Karayigit, A.I.; Bircan, C.; Oskay, R.G.; Türkmen, I.; Querol, X. The geology, mineralogy, petrography, and geochemistry of the Miocene Dursunbey coal within fluvio-lacustrine deposits, Balıkesir (Western Turkey). *Int. J. Coal Geol.* **2020**, *228*, 103548. [CrossRef]
65. Susilawati, R.; Ward, C.R. Metamorphism of mineral matter in coal from the Bukit Asam deposit, south Sumatra, Indonesia. *Int. J. Coal Geol.* **2006**, *68*, 171–195. [CrossRef]
66. Dai, S.; Zhang, W.; Seredin, V.V.; Ward, C.R.; Hower, J.C.; Song, W.; Wang, X.; Li, X.; Zhao, L.; Kang, H.; et al. Factors controlling geochemical and mineralogical compositions of coals preserved within marine carbonate successions: A case study from the Heshan Coalfield, southern China. *Int. J. Coal Geol.* **2013**, *109*, 77–100. [CrossRef]
67. Rao, C.P.; Gluskoter, H.J. Occurrence and Distribution of Minerals in Illinois Coals. *Ill. State Geol. Surv. Circ.* **2015**, *144–145*, 23–47.
68. Dai, S.; Wang, X.; Seredin, V.V.; Hower, J.C.; Ward, C.R.; O'Keefe, J.M.; Huang, W.; Li, T.; Li, X.; Liu, H.; et al. Petrology, mineralogy, and geochemistry of the Ge-rich coal from the Wulantuga Ge ore deposit, Inner Mongolia, China: New data and genetic implications. *Int. J. Coal Geol.* **2012**, *90*, 72–99. [CrossRef]
69. Dai, S.; Liu, J.; Ward, C.R.; Hower, J.C.; Xie, P.; Jiang, Y.; Hood, M.M.; O'Keefe, J.M.; Song, H. Petrological, geochemical, and mineralogical compositions of the low-Ge coals from the Shengli Coalfield, China: A comparative study with Ge-rich coals and a formation model for coal-hosted Ge ore deposit. *Ore Geol. Rev.* **2015**, *71*, 318–349. [CrossRef]
70. Yan, X.; Dai, S.; Graham, I.T.; French, D.; Hower, J.C. Mineralogy and geochemistry of the Palaeogene low-rank coal from the Baise Coalfield, Guangxi Province, China. *Int. J. Coal Geol.* **2019**, *214*, 103282. [CrossRef]
71. Frazer, F.W.; Belcher, C.B. Quantitative determination of the mineral matter content of coal by a radio-frequency oxidation technique. *Fuel* **1973**, *52*, 41–46. [CrossRef]
72. Zhao, L.; Ward, C.R.; French, D.; Graham, I.T. Mineralogy of the volcanic-influenced Great Northern coal seam in the Sydney Basin, Australia. *Int. J. Coal Geol.* **2012**, *94*, 94–110. [CrossRef]

73. Dai, S.; Hower, J.C.; Finkelman, R.B.; Graham, I.T.; French, D.; Ward, C.R.; Eskenazy, G.; Wei, Q.; Zhao, L. Organic associations of non-mineral elements in coal: A review. *Int. J. Coal Geol.* **2020**, *218*, 103347. [CrossRef]
74. Dai, S.; Guo, W.; Nechaev, V.; French, D.; Ward, C.R.; Spiro, B.F.; Finkelman, R.B. Modes of occurrence and origin of mineral matter in the Palaeogene coal (No. 19-2) from the Hunchun Coalfield, Jilin Province, China. *Int. J. Coal Geol.* **2018**, *189*, 94–110. [CrossRef]
75. Zhao, L.; Ward, C.R.; French, D.; Graham, I.T. Mineralogy and major-element geochemistry of the lower Permian Greta Seam, Sydney Basin, Australia. *Aust. J. Earth Sci.* **2013**, *61*, 375–394. [CrossRef]
76. Frey, M. The step from diagenesis to metamorphism in politic rocks during Alpine orogenesis. *Sedimentology* **1970**, *15*, 261–279. [CrossRef]
77. Weaver, C.E.; Broekstra, B.E. illite-mica. In *Shale–Slate Metamorphism in the Southern Appalachians*; Weaver, C.E., Ed.; Elsevier: Amsterdam, The Netherlands, 1984; pp. 67–97.
78. Daniels, E.J.; Altaner, S.P. Inorganic nitrogen in anthracite from eastern Pennsylvania, USA. *Int. J. Coal Geol.* **1993**, *22*, 21–35. [CrossRef]
79. Liu, Q.; Zheng, Q. *Nitrogen in Coal Seam and Nitrogen-Bearing Clay Mineral*; Science Press: Beijing, China, 2016; p. 134. (In Chinese)
80. Dai, S.; Ji, D.; Ward, C.R.; French, D.; Hower, J.C.; Yan, X.; Wei, Q. Mississippian anthracites in Guangxi Province, southern China: Petrological, mineralogical, and rare earth element evidence for high-temperature solutions. *Int. J. Coal Geol.* **2018**, *197*, 84–114. [CrossRef]
81. Dai, S.; Tian, L.; Chou, C.-L.; Zhou, Y.; Zhang, M.; Zhao, L.; Wang, J.; Yang, Z.; Cao, H.; Ren, D. Mineralogical and compositional characteristics of Late Permian coals from an area of high lung cancer rate in Xuan Wei, Yunnan, China: Occurrence and origin of quartz and chamosite. *Int. J. Coal Geol.* **2008**, *76*, 318–327. [CrossRef]
82. Wang, P.; Ji, D.; Yang, Y.; Zhao, L. Mineralogical compositions of the Late Permian coal from the Yueliangtian mine, western Guizhou, China: A comparative study with coals from eastern Yunnan and with an emphasis on the origin of minerals. *Fuel* **2016**, *181*, 859–869. [CrossRef]
83. Xie, P.; Song, H.; Wei, J.; Li, Q. Mineralogical characteristics of Late Permian coals from the Yueliangtian Coal Mine, Guizhou, Southwestern China. *Minerals* **2016**, *6*, 29. [CrossRef]
84. Dai, S.; Chou, C.-L. Occurrence and origin of minerals in a chamosite-bearing coal of Late Permian age, Zhaotong, Yunnan, China. *Am. Miner.* **2007**, *92*, 1253–1261. [CrossRef]
85. Belkin, H.E.; Tewalt, S.J.; Hower, J.C.; Stucker, J.D.; O'Keefe, J.M.K.; Tatu, C.A.; Buia, G. Petrography and geochemistry of Oligocene bituminous coal from the Jiu Valley, Petroşani basin (southern Carpathian Mountains), Romania. *Int. J. Coal Geol.* **2010**, *82*, 68–80. [CrossRef]
86. Ward, C.R. Minerals in bituminous coals of the Sydney Basin (Australia) and the Illinois Basin (U.S.A.). *Int. J. Coal Geol.* **1989**, *13*, 455–479. [CrossRef]
87. Querol, X.; Whateley, M.K.G.; Fernandez-Turiel, J.L.; Tuncali, E. Geological controls on the mineralogy of the Beypazari lignite, central Anatolia, Turkey. *Int. J. Coal Geol.* **1997**, *33*, 255–271. [CrossRef]
88. Finkelman, R.B.; Bostick, N.H.; Dulong, F.T.; Senftle, F.E.; Thorpe, A.N. Influence of an igneous intrusion on the inorganic geochemistry of a bituminous coal from Pitkin County, Colorado. *Int. J. Coal Geol.* **1998**, *36*, 223–241. [CrossRef]
89. Dai, S.; Jiang, Y.; Ward, C.R.; Gu, L.; Seredin, V.V.; Liu, H.; Zhou, D.; Wang, X.; Sun, Y.; Ren, D. Mineralogical and geochemical compositions of the coal in the Guanbanwusu Mine, Inner Mongolia, China: Further evidence for the existence of an Al (Ga and REE) ore deposit in the Jungar Coalfield. *Int. J. Coal Geol.* **2012**, *98*, 10–40. [CrossRef]
90. Dai, S.; Li, D.; Chou, C.-L.; Zhao, L.; Zhang, Y.; Ren, D.; Ma, Y.; Sun, Y. Mineralogy and geochemistry of boehmite-rich coals: New insights from the Haerwusu Surface Mine, Jungar Coalfield, Inner Mongolia, China. *Int. J. Coal Geol.* **2008**, *74*, 185–202. [CrossRef]
91. Chen, Z.; Wu, F.; Zhang, S.; Zhang, N.; Ma, J.; Ge, L. *Sedimentary Environments and Coal Accumulation of Late Paleozoic Coal Formation in Northern China*; Press of China University of Geosciences: Beijing, China, 1993; p. 190. (In Chinese)